Microanalysis of silver jewellery by laser-ablation laser-induced breakdown spectroscopy with enhanced sensitivity and minimal sample ablation

Junyu Mo (磨俊宇), Yuqi Chen (陈钰琦), Runhua Li (李润华)*, Qi Zhou (周 奇), and Yang Lou (楼 洋)

Department of Physics, School of Science, South China University of Technology, Guangzhou 510641, China

**Corresponding author: rhli@scut.edu.cn*

Received March 1, 2014; accepted May 20, 2014; posted online July 18, 2014

Laser-ablation laser-induced breakdown spectroscopy (LA-LIBS) based on single Nd:YAG laser is used to analyze copper impurity in silver jewellery with enhanced sensitivity and minimal sample ablation. 6-30 folds signal enhancement can be achieved under the re-excitation of the breakdown laser and the spatial resolution is only determined by the ablation laser. 50 ppm limit of detection of copper is achieved when the crater diameter is 17.2 μm under current experimental condition. This technique gives higher analysis sensitivity under the same sample ablation in comparison with single pulse (SP) LIBS. It is useful for high sensitive element microanalysis of precious samples.

OCIS codes: 300.6365, 300.6210, 300.6190.
doi: 10.3788/COL201412.083001.

Laser-induced breakdown spectroscopy (LIBS) is able to provide an accurate, *in-situ*, and quantitative chemical analysis with good sensitivity and spatial resolution. With the development of laser and optoelectronic detection technologies, the application of LIBS has already been extended to more and more fields in the past decades. For example, LIBS has been used to analyze total nitrogen and phosphorus and heavy metals in soil[1,2]. On multi-elements analysis of precious samples, LIBS has been used to determine the provenance of different gem stones and to characterize different jewelleries[3−5]. Quantitative analysis of gold and silver alloys by LIBS has also been reported in literatures[6−9]. LIBS is also applied in the fields of archaeology and art; the analyzed samples include historic metal artifacts[10], ordnance[11], Roman silver denarii[12], ancient ceramics[13], fresco[14], and pigments on painted plasters[15]. The common requirement in precious sample analysis mentioned above was the sample ablation during the analysis had to be minimal. In other words, the spatial resolution of LIBS should be as high as possible.

However, there is a contradiction between analytical sensitivity and spatial resolution in conventional single-pulse (SP) LIBS because the sample ablation and breakdown are completed by the same laser pulse. In SP-LIBS, higher analytical sensitivity usually requires higher laser energy; on the contrary, higher laser energy will create bigger craters on the sample surface and deteriorate the spatial resolution. Thereafter, it is difficult to analyze trace elements in the sample with SP-LIBS if high spatial resolution is required at the same time.

Different efforts have been made to solve this problem. The first one was the combination of laser-induced fluorescence (LIF) and LIBS, in which the atoms produced in the laser-induced plasma were resonantly excited by the second laser and the LIFs of the atoms were monitored for high sensitive analysis[16−18]. Chan *et al.* reported an interesting method to enhance atomic emission of the laser-induced plasma, which was termed with resonance-enhanced laser-induced plasma spectroscopy (RELIPS). In their work, the potassium atoms were resonantly photoionized by a second laser beam and the sodium emission at 589 nm was enhanced[19]. The techniques of LIF+LIBS and RELIPS are both able to reduce sample ablation under the same analytical sensitivity in comparison with SP-LIBS due to the enhanced atomic emissions. However, these techniques require a tunable laser to realize resonant excitation of the atoms in the plasma.

Dual-pulse (DP) LIBS based on two Nd:YAG lasers has been established to enhance analytical sensitivity of LIBS in the past decades[20−24]. There are three types of geometrical arrangements for DP-LIBS: collinear, cross beam, and orthogonal. The orthogonal DP-LIBS can be further classified as pre-ablative[24] and reheating[21,23] DP-LIBS according to different interpulse time delays. To achieve better analytical performance, DP-LIBS with different laser combinations, such as excimer laser plus Nd:YAG laser[25], CO_2 laser plus Nd:YAG laser[26], femtosecond Ti:Sapphire plus Nd:YAG lasers have also been studied[27]. In most of the DP-LIBS studies mentioned above, researchers paid less attention on spatial resolution improvement than on signal enhancement and two laser systems were usually required. Antony *et al.*[28] reported a cross beam DP-LIBS for analysis of lunar simulant samples in which only single Nd:YAG laser was required. In their experiment, 532-nm laser from one Nd:YAG laser was used to ablate sample and 1064-nm laser from the same laser was used to reheating the plasma to get enhance plasma emission.

This letter will report an application of orthogonal dual-wavelength dual-pulse laser-ablation LIBS (ODWDP LA-LIBS) on the microanalysis of copper impurity in silver jewellery based on single Nd:YAG laser. In this technique, the 532-nm laser pulse from a *Q*-switched Nd:YAG laser was used to ablate small amount of samples and the 1064-nm laser pulse from the same laser was used to break down the ablated samples for spectral analysis. The propagation directions of these

two pulses were geometrically orthogonal. The analytical performance of this technique and its possible applications will be discussed.

The experimental setup of ODWDP LA-LIBS is schematically shown in Fig. 1. A Q-switched Nd:YAG laser with 12-ns pulse width and 5-Hz repetition rate was used in the experiments. The second harmonic output (532 nm) of the Nd:YAG laser was chosen as ablation laser source since shorter wavelength was helpful to achieve higher spatial resolution. The 532-nm laser beam was focused on the sample surface by a 50× long-working distance microscopic objective (MO) with 0.42 numerical aperture (NA) and 20.5 mm working distance after passing through a dichromatic beam splitter (BS) and two Glan-Taylor linear polarizers. The propagation direction of 532 nm laser beam was perpendicular to sample surface. The first polarizer (P1) was used to obtain linear polarized light and the second linear polarizer (P2) was used to attenuate laser pulse energy by rotating its polarization direction in respect to that of P1. Thus the polarization direction of the 532-nm laser changed with pulse energy variation in the experiments. This polarization change would not bring any difference in laser-ablation process for the studied samples.

The fundamental output (1064 nm) from the same Nd:YAG laser was reflected by two right angle prisms and then focused by a 4× microscopic objective (L1) with 0.10 NA and 32-mm focal length. The propagation direction of 1064-nm laser beam was parallel with sample surface. The focus center of the 1064-nm laser should be very close to sample surface but the sample ablation by 1064-nm laser should be avoided. The distance from focus center of the 1064-nm laser to sample surface was experimentally optimized by monitoring atomic emission of silver atoms under DP (532+1064 nm) excitation and SP (1064 nm only) excitation. Silver atomic emission should not be observed if the 532-nm laser was blocked. The time delay of 1064-nm laser pulse to 532-nm laser pulses was determined by optical length from BS to prism 1 and prism 2 to the sample. Since the beam diameter of the 1064-nm laser would expand so much after long transmission distance, this would lose most of the pulse energies due to the limited aperture of the focusing objective. Therefore, only 2-ns time delay was adopted in all the following experiments.

The analyzed samples were silver finger rings cut to the size of 1×3×20 (mm). The sample was mounted on a two-dimensional (2D) translation platform and kept moving at the speed of 180 μm/s to ensure each laser shot on different places on sample surface during the experiment. The short width (3 mm) of the sample was chosen to avoid the clipping effect of the sample to the light propagation of the focused 1064-nm laser beam.

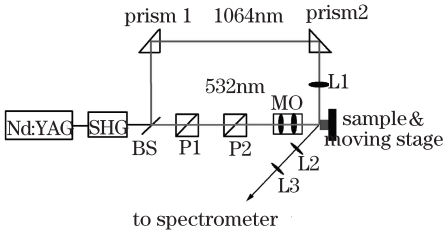

Fig. 1. (Color online) Experimental setup of ODWDP LA-LIBS based on single Nd:YAG laser. P1 and P2: Glan-Taylor linear polarizer; L1: 4× objective; L2 and L3: quartz lens.

The emission of the laser-induced plasma was collected by quartz lens L2 and then focused on to the entrance slit of a spectrometer by quartz lens L3. The spectrometer consisted of a monochromator for wavelength selection, a 250-MHz digital storage oscilloscope for signal collection and a personal computer for data process and wavelength scanning. For each laser shot, the emission waveform of the plasma at selected wavelength could be detected by a photomultiplier tube and recorded by the digital storage oscilloscope. Then the waveform data saved in the oscilloscope were transferred to the personal computer via a GPIB interface. The detailed information about signal recording and data process could be found in previous publication[29].

Two silver finger rings were analyzed with ODWDP LA-LIBS. The concentrations of copper in the jewellery were determined to be 3.06% and 0.07% with atomic absorption spectrometer (AAS).

When the sample was ablated by 532-nm laser pulse with low pulse energy, the ablated sample was also broken down at the same time, a very weak atomic emission with short time duration could be observed experimentally. Therefore, the LA process could also be treated as SP-LIBS under low laser pulse energy.

Figure 2 shows a comparison of the temporal profiles of the silver atomic emission at 328.07 nm and the plasma background emission at 328.6 nm obtained under three different excitation conditions: ODWDP LA-LIBS with 532+1064-nm laser pulses, LA with only 532-nm laser pulse, and LIBS with only 1064-nm laser pulse. The pulse energies of 532-nm laser and 1064-nm laser used in experiment were 300 μJ and 16 mJ respectively and the concentration of copper in the sample was 3.06%. The

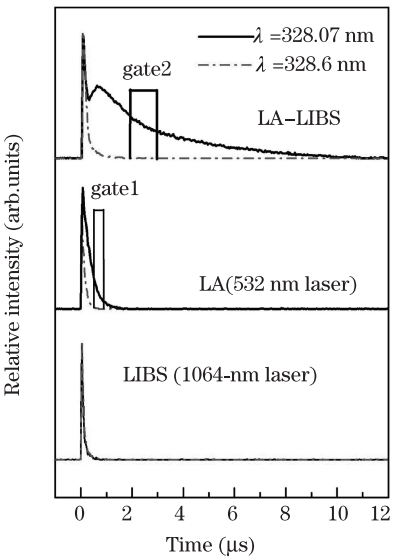

Fig. 2. (Color online) Temporal profiles of silver atomic emission at 328.07 nm and plasma background emission at 328.6 nm under different excitation conditions. Top: LA-LIBS with 532+1064-nm laser pulses; middle: LA with 532-nm laser pulse; bottom: LIBS with 1064-nm laser pulse. Data acquisition gates selected for spectra collection in LA-LIBS and LA were also shown in this figure.

temporal profiles were recorded with the digital oscilloscope. The waveforms had been averaged for 150 laser shots to get better signal to noise ratio.

In LA with 300-μJ, 532-nm pulse energy, weak silver atomic emission with about 2-μs time duration could be observed. When 16-mJ, 1064-nm laser pulse was brought in to break down the ablated samples, the atomic emission of silver was significantly enhanced and its time duration was extended to about 10 μs. However, the time duration of the background emission in LA-LIBS was shorter than 2 μs. This was very helpful to realized time-resolved detection to get higher signal to background ratio. The bottom part in Fig. 2 shows the plasma emission due to air breakdown under the excitation of only 1064-nm laser. The recorded plasma emissions at two wavelengths were similar, and there were no silver atomic emissions could be observed. This provided a direct experimental proof to demonstrate that the 1064-nm laser did not ablate any new samples and the enhanced silver atomic emission observed in LA-LIBS was coming from the samples ablated by 532-nm laser pulse.

Emission spectra in the wavelength region of 323–340 nm recorded in LA and LA-LIBS are shown in Fig. 3. The data acquisition gate was set at 0.4–1.0 μs in LA and at 2.0–3.0 μs in LA-LIBS, respectively. Significant signal enhancement for silver, copper, and zinc atomic emissions were achieved simultaneously in LA-LIBS in comparison with in LA, or SP-LIBS.

Supposing the fluency distribution in the focal plan is Gaussian, the ablation threshold of the sample is $F_{\rm t}$, the function of pulse energy (E) to the radius of the crater ($r_{\rm t}$) can be derived as[30]

$$E = F_{\rm t}\frac{\pi}{2}w^2 e^{2r_{\rm t}^2/w^2}, \tag{1}$$

where w is the spot size of the focus on the focal plan, thus,

$$r_{\rm t} = \frac{\sqrt{2}}{2}w\sqrt{\ln\left(\frac{2E}{\pi F_{\rm t}w^2}\right)}. \tag{2}$$

This indicates that the crater diameter will decrease if the pulse energy used for ablation decreases.

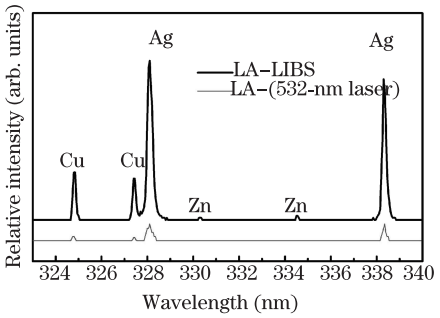

Fig. 3. (Color online) Emission spectra of the plasma in 323–340 nm wavelength region recorded in LA-LIBS and LA. Up: LA-LIBS with 532+1064-nm laser pulses; down: LA with 532-nm laser pulse. Pulse energies of 532-nm laser and 1064-nm laser were 300 μJ and 16 mJ, respectively.

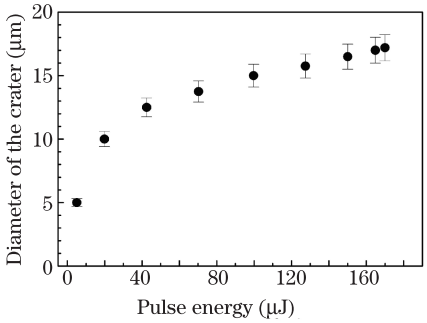

Fig. 4. Plot of the crater diameter versus pulse energy of the 532-nm laser.

Figure 4 shows a plot of crater diameter versus pulse energy of 532-nm laser determined experimentally. The pulse energy of 532-nm laser was attenuated gradually by rotating the polarization plan of the second linear polarizer P2. The crater diameter was measured with an optical microscope. Averaged results of both craters' diameter and pulse energy were taken from multiple measurements to ensure good accuracy. The maximum diameter was 17.2 μm when ablation pulse energy was 170 μJ and the minimum diameter was 5 μm when ablation pulse energy was only 5.1 μJ.

To ensure high spatial resolution of the microanalysis or to minimize sample ablation, the ablation from 1064-nm laser had to be avoided. The way to realize this was moving the focus of 1064-nm laser away from sample surface carefully and monitoring plasma emission when the 532-nm (ablation) laser was blocked until silver atomic emission disappeared thoroughly, just as shown at the bottom of Fig. 2. The craters created by 532-nm laser and 532+1064-nm lasers under this condition were checked under scanning electron microscope (SEM) and there were no observable difference could be found. When the 532-nm laser was blocked and the air in front of sample surface was broken down only by 1064-nm laser pulse, without any created crater could be observed under SEM. These demonstrated again that, at the optimized distance from focus center of 1064-nm beam to the sample surface, the breakdown (1064 nm) laser did not participate in any ablation process when the atomic emissions of the samples were significantly enhanced. Therefore, the second laser pulse only broken down the samples ablated by 532-nm laser, thus the spatial resolution or sample ablation in ODWDP LA-LIBS was only determined by the ablation (532 nm) laser.

The signal enhancement factors of copper atomic emission at 324.75 nm and silver atomic emission at 328.07 nm obtained after 1064 nm laser excitation under different spatial resolutions are listed in Table 1, while the peak atomic line intensities in wavelength spectra are used for this evaluation. In the experiments, the pulse energy of 1064-nm laser was fixed at 16 mJ and the pulse energy of 532-nm laser was varied. Limited by the detection sensitivity of current system, the atomic emission signals of copper and silver were too weak to be detected in LA when the pulse energy of 532-nm laser was lower than 70 μJ, thus the enhancement factors were temporarily unavailable. It is easy to find that the enhancement factor obtained at low ablation laser energy is

Table 1. List of Signal Enhancement Factors of Copper Emission at 324.75 nm and Silver Emission at 328.07 nm Obtained in ODWDP LA-LIBS (532+1064 nm) in Comparison with that Obtained in LA (532 nm) under Different Pulse Energies of 532-nm Laser, Pulse Energy of 1064-nm Laser used was 16 mJ.

Pulse Energy of 532-nm Laser (μJ)	Diameter of Crater (μm)	Signal Enhancement Factor for Copper Emission at 324.75 nm	Signal Enhancement Factor for Silver Emission at 328.07 nm
170	17.2	6.9	6.5
165	17.0	7.6	9.9
150	16.5	17.6	12.7
128	15.8	28.2	29
100	15.0	30.2	32
70	13.8	–	–

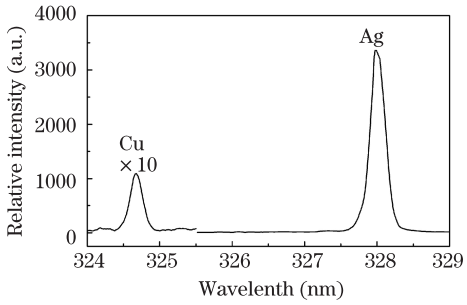

Fig. 5. Emission spectrum between 323–329 nm obtained in ODWDP LA-LIBS by analyzing the second sample in which copper concentration was 700 ppm. The pulse energies of 532- and 1064-nm laser beams used in the experiments were 170 μJ and 16 mJ, respectively.

higher than that obtained at high ablation laser energy. This characterization of the ODWDP LA-LIBS is especially important for high spatial resolution microanlaysis for solid samples.

In order to estimate the limit of detection (LOD) of copper in ODWDP LA-LIBS technique under current experimental conditions, the second sample (C_{Copper}=0.07%) was analyzed with this technique. Since the concentration of copper in this sample is only 700 ppm, the self-absorption effect of the resonant line at 324.78 nm can be ignored. Figure 5 shows an emission spectrum in the wavelength of 323–329 nm of this sample. The data acquisition gate was the same as that shown in Fig. 2. The pulse energies of 532- and 1064-nm laser beams used in the experiments were 170 μJ and 16 mJ, respectively and the crater diameter was about 17.2 μm. The LOD of copper in silver matrix estimated according to 3σ rule (LOD=3σ/s) was about 50 ppm in ODWDP LA-LIBS technique under current experimental condition. The standard deviation of the background σ was estimated based on the background noise in the wavelength region of 325–325.5 nm.

There are three new features in current ODWDP LA-LIBS technique: firstly, this technique ensures both high spatial resolution and high sensitivity in comparison with SP-LIBS. Therefore, it is possible to reduce the mass ablation under the same analytical sensitivity in ODWDP LA-LIBS than in SP-LIBS. Secondly, only single Nd:YAG laser is used in current system which simplifies the requirement for laser systems and electronic control unit for interpulse delay in comparison with traditional DP-LIBS technique and combination technique of LIF and LIBS. Thirdly, the atomic emissions of multielements are able to be enhanced simultaneously under the excitation of 1064-nm laser pulse. However, in the technique of LIF+LIBS, atomic emissions coming from only one upper level can be enhanced by the re-excitation of the second laser.

It is worthwhile to compare Antony's work reported in Ref. [28] with this work. Although both works adopted 532+1064-nm wavelength combination based on single Nd:YAG laser, 1064-nm laser certainly contributed to sample ablation thus deteriorate the spatial resolution in Antony's work due to cross beam geometrical arrangement; however, in this work, 1064-nm laser did not ablate any samples during the reheating process, this ensured a high spatial resolution which was only determined by 532-nm laser due to orthogonal geometrical arrangement.

Continuous works on further improving the spatial resolution and analytical sensitivity are undergoing in our laboratory, such as adopting 266-nm laser pulse as ablation source, using new objectives to get smaller focal spot and recording weak plasma emissions with photon counting technique.

In conclusion, microanalysis of copper impurities in silver jewellery by ODWDP LA-LIBS can be realized base on single Nd:YAG laser. In this technique, significant signal enhancement can be achieved under the re-excitation of the breakdown laser and the spatial resolution is only determined by the ablation laser. A LOD of 50 ppm for copper in silver matrix is achieved when crater diameter is controlled at 17.2 μm under current experimental condition. This technique ensures both high sensitivity and high spatial resolution in comparison with single pulse LIBS. It is especially useful to element analysis of precious samples, such as gems, jewellery, cultural relics, and artworks, etc., in which minimal sample ablation or high spatial resolution is usually required.

This work was financially supported by the National "973" Program of China (No. 2012CB921900), the National Natural Science Foundation of China (Nos. 11274123 and 11304100), and the Basic Scientific Research Program of South China University of Technology (No. 2014ZZ0066).

References

1. C. Lu, L. Wang, H. Hu, Z. Zhuang, Y. Wang, R. Wang, and L. Song, Chin. Opt. Lett. **11,** 053004 (2013).
2. C. Xie, J. Lu, P. Li, J. Li, and Z. Lin, Chin. Opt. Lett. **7,** 060545 (2009).
3. C. E. McManus, N. J. McMillan, R. S. Harmon, R. C. Whitmore, F. C. De Lucia, and A. W. Miziolek, Appl. Opt. **47,** G72 (2008).
4. L. E. Garcia-Ayuso, J. Amador-Hernandez, J. M. Fernandez-Romero, and M. D. L. de Castro, Anal. Chim. Acta **457,** 247 (2002).
5. A. Jurado-López and M. D. L. de Castro, J. Anal. At. Spectrom. **17,** 544 (2002).

6. V. S. Burakov and S. N. Raikov, Spectrochim. Acta Part B **62,** 217 (2007).
7. G. Galbács, N. Jedlinszki, G. Cseh, Z. Galbács, and L. Túri, Spectrochim. Acta Part B **63,** 591 (2008).
8. S. Pandhija and A. K. Rai, Pramana-J. Phys. **70,** 553 (2008).
9. B. Rashid, R. Ahmed, R. Ali, and M. A. Baig, Phys. Plasmas **18,** 073301 (2011).
10. K. Melessanaki, M. Mateo, S. C. Ferrence, P. P. Betancourt, and D. Anglos, Appl. Surf. Sci. **197-198,** 156 (2002).
11. S. Acquaviva, M. L. De Giorgi, C. Marini, and R. Poso, J. Cult. Herit. **5,** 365 (2004).
12. L. Pardini, A. El Hassan, M. Ferretti, A. Foresta, S. Legnaioli, G. Lorenzetti, E. Nebbia, F. Catalli, M.A. Harith, D. D. Pace, F. A. Garcia, M. Scuotto, and V. Palleschi, Spectrochim. Acta Part B **74-75,** 156 (2012).
13. F. Colao, R. Fantoni, V. Lazic, and V. Spizzichino, Spectrochim. Acta Part B **57,** 1219 (2002).
14. L. Caneve, A. Diamanti, F. Grimaldi, G. Palleschi, V. Spizzichino, and F. Valentini, Spectrochim. Acta Part B **65,** 702 (2010).
15. P. Westlake, P. Siozos, A. Philippidis, C. Apostolaki, B. Derham, A. Terlixi, V. Perdikatsis, R. Jones, and D. Anglos, Anal. Bioanal. Chem. **402,** 1413 (2012).
16. F. Hilbk-Kortenbruck, R. Noll, P. Wintjens, H. Falk, and C. Becker, Spectrochim. Acta Part B **56,** 933 (2001).
17. S. L. Lui, Y. Godwal, M. T. Taschuk, Y. Y. Tsui, and R. Fedosejevs, Anal. Chem. **80,** 1995 (2008).
18. X. K. Shen, H. Wang, Z. Q. Xie, Y. Gao, H. Ling, and Y. F. Lu, Appl. Opt. **48,** 2551 (2009).
19. S. Y. Chan and N. H. Cheung, Anal. Chem. **72,** 2087 (2000).
20. J. Scaffidi, S. M. Angel, and D. A. Cremers, Anal. Chem. **78,** 24 (2006).
21. Q. Wang, F. Z. Dong, Y. X. Liang, X. L. Chen, J. G. Wang, B. Wu, and Z. B. Ni, Acta Opt. Sin. (in Chinese) **31,** 1030002 (2011).
22. L. B. Guo, B. Y. Zhang, X. N. He, C. M. Li, Y. S. Zhou, T. Wu, J. B. Park, X. Y. Zeng, and Y. F. Lu, Opt. Express **20,** 1436 (2012).
23. R. W. Coons, S. S. Harilal, S. M. Hassan, and A. Hassanein, Appl. Phys. B **107,** 873 (2012).
24. C. Du, X. Gao, Y. Shao, X. W. Song, Z. M. Zhao, Z. Q. Hao, and J. Q. Lin, Acta Phys. Sin. (in Chinese) **62,** 045202 (2013).
25. X. N. He, W. Hu, C. M. Li, L. B. Guo, and Y. F. Lu, Opt. Express **19,** 10997 (2011).
26. R. W. Coons, S. S. Harilal, S. M. Hassan, and A. Hassanein, Appl. Phys. B **107,** 873 (2012).
27. J. Scaffidi, W. Pearman, M. Lawrence, J. C. Carter, B. W. Colston, and S. M. Angel, Appl. Opt. **43,** 5243 (2004).
28. J. K. Antony, N. J. Vasa, V. L. N. Sreedhar Raja, and A. S. Laxmiprasad, J. Phys. D: Appl. Phys. **45,** 365401 (2012).
29. Z. J. Chen, H. K. Li, F. Zhao, and R. H. Li, J. Anal. At. Spectrom. **23,** 871(2008).
30. Q. Zhou, Y. Q. Chen, F. F. Peng, X. J. Yang, and R. H. Li, Appl. Opt. **52,** 5600 (2013).